Talanta 116 (2013) 474–481

Contents lists available at ScienceDirect

Talanta

journal homepage: www.elsevier.com/locate/talanta

Trace detection of oxygen – ionic liquids in gas sensor design

N. Baltes*, F. Beyle, S. Freiner, F. Geier, M. Joos, K. Pinkwart, P. Rabenecker

Fraunhofer Institut für Chemische Technologie, Joseph-von-Fraunhofer-Str. 7, D-76327 Pfinztal (Berghausen), Germany

ARTICLE INFO

Article history:
Received 12 March 2013
Received in revised form
27 June 2013
Accepted 2 July 2013
Available online 11 July 2013

Keywords:
Ionic liquids
Tetracyanoborates
Oxygen
Temperature behaviour
Electrochemical sensor
Trace analysis

ABSTRACT

This paper presents a novel electrochemical membrane sensor on basis of ionic liquids for trace analysis of oxygen in gaseous atmospheres. The faradaic response currents for the reduction of oxygen which were obtained by multiple-potential-step-chronoamperometry could be used for real time detection of oxygen down to concentrations of 30 ppm. The theoretical limit of detection was 5 ppm. The simple, non-expensive sensors varied in electrolyte composition and demonstrated a high sensitivity, a rapid response time and an excellent reproducibility at room temperature. Some of them were continuously used for at least one week and first results promise good long term stability. Voltammetric, impedance and oxygen detection studies at temperatures up to 200 °C (in the presence and absence of humidity and CO_2) revealed also the limitations of certain ionic liquids for some electrochemical high temperature applications.

Application areas of the developed sensors are control and analysis processes of non oxidative and oxygen free atmospheres.

1. Introduction

A highly sensitive oxygen sensor is a key parameter of many process-control systems. They are needed to monitor flammable or explosive gas mixtures, to control strictly inert gas atmospheres in semiconductor, nuclear or life science industries as well as to ensure efficient combustion. In the latter case, they must be able to operate at different elevated temperatures. Gas sensors in general very often measure the change of resistance of a metal oxide surface or they work as field effect transistors [1–8]. As the surface conductivity is influenced not only by temperature but easily by several gases these sensors often need an analyte separation and, hence, serve as gas detectors e.g. in gas chromatography devices. Another popular metal oxide sensor is the oxygen sensitive lambda sensor. Its working temperature is, however, in the range of several hundred centigrades and should be kept at a constant level. An alternative to measure the oxygen content of some gas at lower temperatures is the Clark electrode. Yet, the temperature range of this sensor is fixed between 0 and 100 °C because of the aqueous electrolyte.

Ionic liquids (IL), ionic compounds that have melting points of 100 °C or below, show a high chemical stability, a relatively wide potential window and a good ionic conductivity. Furthermore, they have a negligible vapour pressure even at elevated temperatures, as a result of which they are considered to be uninflammable (for a review see Ref. [9–11]). Hence, in electrochemistry ILs have been assesed as an interesting, save and temperature stable electrolyte over the last decade. Moreover, specific gas solubilities of ILs are different from liquid to liquid. In comparison to the classical Clark electrode, it is on account of the great number of cations and anions that ILs suggest great promise for an improvement of sensor selectivity and reduction of any cross-sensitivities (apart from an enhanced applicability at higher temperatures because of the thermal stability of the ILs).

A number of papers have been published within the recent years describing diffusion, solubility and general electrochemical behaviour of oxygen in different ILs [12–26]. The electrochemical investigations went hand in hand with the development and characterisation of potential oxygen sensors using ILs as electrolyte and microdisk electrodes [13,14], classical membrane [27] or membrane free [28–30] designs. Wang et al. elucidated the strong influence of water on a IL-membrane sensor and used steady state as well as transient currents for evaluating different sorts of calibration plots [31,32]. Another oxygen sensitive amperometric IL-sensor which based on the principles of the Clark electrode was presented by Wang et al. [27] Most measurements were performed at room temperature between 10 and 100 vol% oxygen. (Jin et al. presented a rare high-temperature sensor to detect organic vapours, by depositing thin IL-films on a quartz crystal microbalance and relating weight dependent frequency changes to dissolution of the vapours into the IL [33].)

The Clark type sensor showed a limit of detection of 0.28 vol%, but to our knowledge there have not been any voltammetric quantifications in the ppm-range and/or at elevated temperatures.

---

* Corresponding author. Tel.: +49 721 4640 868; fax: +49 721 4640 318.
E-mail address: norman.baltes@ict.fraunhofer.de (N. Baltes).

0039-9140/$ - see front matter © 2013 Elsevier B.V. All rights reserved.
http://dx.doi.org/10.1016/j.talanta.2013.07.001

The general idea of this paper is to use temperature-stable and non-volatile ionic liquids as electrolytes in order to develop an oxygen sensor for application in the range of ppm concentrations which might be also able to measure in temperature ranges greater than 100 °C.

2. Experimental

2.1. Reagents

The following ILs were purchased from Iolitec, Germany: 1-ethyl-3-methylimidazolium bis(trifluoromethylsulfonyl)imide (EMIM NTf_2), 1-hexyl-3-methylimidazolium bis(trifluoromethylsulfonyl) imide (HMIM NTf_2), 1-methyl-3-octylimidazolium bis(trifluoromethylsulfonyl)imide (OMIM NTf_2) and trihexyl-(tetradecyl) phosphonium bis(trifluoromethylsulfonyl)imide ($P_{6,6,6,14}$ NTf_2). 1-Hexyl-3-methylimidazolium tris(pentafluoroethyl)trifluorophosphate (HMIM FAP), 1-ethyl-3-methylimidazolium tetracyanoborate (EMIM TCB), 1-butyl-3-methylimidazolium tetracyanoborate (BMIM TCB) and 1-hexyl-3-methylimidazolium tetracyanoborate (HMIM TCB) were produced by the Merck Company, Germany. All chemicals were used without further purification (specification of the supplier: water (KF) $<$ 100 ppm, halides $<$ 100 ppm). Sulphuric acid was purchased from Roth, Germany, and diluted using Milli-Q water.

2.2. Electrochemical system

Cyclic voltammograms (CVs) were recorded on a VMP 3 (BioLogic) instrument using a standard three electrode cell comprised of a glassy carbon (GC) electrode (Metrohm) as working electrode, Pt-wire as counter electrode and a Pt or a silverchloride covered Ag-wire as quasi reference electrode. In case of using Pt-working electrodes, the working electrode was a Pt-disk sealed in soft glass (0.5 mm diameter). A Pt-wire, wrapped around the glass of the working electrode, was used as the counter-electrode [34]. The working electrode was polished with 6, 1 and 0.5 μm diamond paste (Buehler) and activated by potential cycling in 0.5 mol/L sulphuric acid. The conductivities of the ionic liquids were measured by the standard complex impedance method, using the same VMP 3 potentiostat in the frequency range from 0.5 Hz to 60 kHz. A conventional sealed diptype electrode (Metrohm, Germany) was employed. The cell constants were about $0.8\ cm^{-1}$, calibrated with a 0.1 mM KCl aqueous solution. Voltammetric and impedance measurements were made during controlled slow heating from 20 to 220 °C in a classical electrochemical cell under a blanket of argon or, if mentioned, in an argon-filled glove box (Braun, O_2 and $H_2O < 5$ ppm) in Ar-atmosphere.

2.3. Sensor preparation

The sandwich type membrane gas sensor consisted of two different alumina microfiltration membranes (Kerafol, porediameter: 80 nm, thickness: 2 mm and Innocermic, porediameter: 400 nm, thickness: 1 mm, d_{50}: 3 μm) separated by a Pt or Au working electrode respectively, a counter and reference electrode of the same metal (see Fig. 1). All electrodes were made of 99.99% metal foils ($1.5 \times 15.0 \times 0.025$ mm, Goodfellow, UK) or flattened metal wires of a diameter of 0.5 mm. The less than millimeter-sized gap between the two membranes was filled with electrolyte after fixation of the membrane-electrode arrangement by chemical inert glass colour (Wolbring, Germany), which was baked at 700 °C for 15 min.

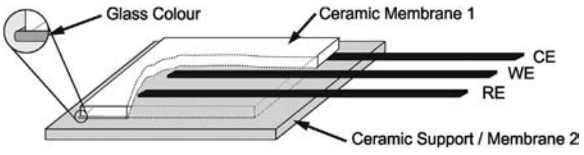

Fig. 1. Schematic drawing of a typical membrane sensor. WE: working electrode; RE: reference electrode; CE: counter electrode.

2.4. Apparatus

The sensor was fixed in a ½″ tube of stainless steel acting as test chamber inside a tube furnace (Horst, Germany). Mass flow controllers by MKS Instruments Deutschland GmbH, Germany, maintained a constant and controlled gas release and adjusted defined gas concentrations. They were connected with the test chamber by means of ¼″ tubings of stainless steel (Swagelog, Germany) which were heated by heating bands (Mohr & Co., Germany). A controlled humidification was allowed by an alternative bypass through a membrane gas humidifier (Perma Pure, MH-070, 48″ by Ansyco, Germany). The gas stream (argon 5.0 (carrier gas); oxygen 6.0 and CO_2 4.5 by Westfalen, Germany) was finally lead into a wash bottle filled with silicone oil in order to prevent gas getting into the device from outside. The gas composition was controlled online by a mass spectrometer (Pfeiffer, QMG 700, Germany) referring all signals to the main signal of the carrier gas.

3. Results and discussion

3.1. Electrochemical and thermal characterisation

Many ILs are hygroscopic. As the electrolyte of a sensor is in permanent equilibration with the surrounding humidity, swelling and, therefore, leaking effects could be the consequence. Furthermore, absorbed moisture changes the electrochemical window and the viscosity of the IL, which in turn affects the diffusional transport and results in irreproducible currents [14]. Hence, hydrophobic ILs containing NTf_2, TCB or FAP anions, which tend to be highly fluid, thermal and hydrolytic stable [35–39] are promising electrolyte candidates.

Electrochemical stability of several ILs was determined using cyclic voltammetry at Pt-electrodes vs. Pt-quasi reference electrode (Pt-QRE) in a temperature range between 20 °C and 220 °C. The scans were always recorded first in anodic direction. Fig. 2 shows the dependency of the potential window of OMIM NTf_2 on the temperature. In comparison to cyclic voltammograms (CVs) of the same IL recorded at GC electrodes (see Fig. 2a) the corresponding CVs recorded at Pt-electrodes (Fig. 2b) show a smaller potential window especially at elevated temperatures. At 120 °C, the electrochemical window showed a range of 2.65 V using Pt-electrodes and 3.88 V using GC electrodes. As the irreversible reduction of the organic cations is apparently promoted at higher temperatures, the cathodic limit decreases at both the GC and Pt-electrodes. On the other hand, the anodic limit, at which a decomposition of the anions is generally observed, remains rather stable at the GC but decreases at the Pt-electrodes. (A good part of literature concerning oxygen reduction in ILs is based upon measurements by means of GC electrodes. Therefore, the herewith presented results offer a good possibility to compare the totally different properties of these two electrode materials with each other and with literature data. However, as fixation and luting of the sensor were conducted by means of chemically inert glass colour at temperatures of several hundred degrees centigrade, it was not possible to use GC as sensor electrode material.)

A general trend of a smaller potential window at higher temperatures could be observed in all ILs. Moreover, it could be confirmed that the electrochemical window is strongly affected by impurities [40] especially water [41–44]. Additional peaks and shoulders appearing in the CV at higher temperatures as well as brownish films on top of the electrode surface indicate that many ILs start to react irreversibly at Pt-electrodes, especially in the presence of traces of water. Owing to this a series of CVs at different temperatures might become hardly reproducible without purification of the electrode and the IL.

Conductivity measurements between 20 and 220 °C (presented in Fig. A in the additional information) show a drastic (10-fold) enhancement of the conductivity. Especially the ILs consisting of the small TCB anion are characterised by a comparatively high conductivity (EMIM-TCB: 20–220 °C; 10–130 mS cm^{-1}).

Hence, it has to be considered from case to case, in dependency on the temperature, the electrochemical window, the electrode material and the redox potential of the analyte which IL might be most suitable to serve as electrolyte under the given circumstances. Here, basic studies were performed using HMIM FAP, EMIM TCB, EMIM NTf_2 and $P_{6,6,6,14}$ NTf_2, since they all showed no noticeable voltammetric features in the absence of oxygen when fully purged under vacuum.

3.2. *Oxygen detection*

Several cyclic voltammetric experiments dealing with oxygen reduction in various ILs have already been described in literature. They gave first informations about oxygen solubilities, diffusion and charge transfer coefficients or activation energies for diffusion of oxygen. Most of them have been performed by means of GC electrodes in dry ILs after sparging with oxygen[16,45–47]. An extensive comparison between experimental results at Pt, Au and GC ultramicroelectrodes (UMEs) and theoretical data has been carried out in Comptons group [15,21–24].

In such works, the UMEs as well as the reference electrode were covered by an IL drop and positioned in a gas stream. The limiting current measured at the UMEs showed a linear behaviour in dependence of the concentration which was usually in the range of 10–100 vol%.

In this paper we present measurements in the ppm range obtained by a sandwich like membrane sensor containing either Au-or Pt-electrodes. All sensors were handled under normal lab conditions and finally enclosed in a gas pipe in order to measure in gas streams of different compositions or temperatures.

Typical CVs recorded by means of an IL-membrane-sensor differ very much from the classical CV obtained directly in the IL. Diffusional transport through the membrane as well as the simple fact that the completely enclosed electrodes cannot be repolished and purified after electrode poisoning reactions must be taken into account. A common CV recorded in oxygen saturated HMIM FAP by means of a classical, fresh polished Pt-electrode showed an irreversible cathodic peak at −1.53 V which is caused by the reduction of oxygen to superoxide as well as an anodic peak at about −0.99 V (see Fig. B in the supplementary data). The peak seperation of 540 mV is generally assigned to different diffusion coefficients of the neutral oxygen species (fast diffusion) and the charged superoxide anion (slow diffusion). This effect might be particular noticeable in imidazolium ILs because of strong ion-pairing between superoxide and imidazolium ions [21,23,25].

A corresponding CV obtained using a Pt-membrane-sensor (filled with HMIM FAP) is exemplified in Fig. 3a. Here, the sensor was placed in a gas stream of argon (dotted line) or a mixture of argon and 0.1% oxygen (straight line). The beginning of an ill-defined reduction wave, starting at −0.6 V was detected in the presence of oxygen. In the absence of oxygen only a normal background current of the ionic liquid is observed. The vertex potentials were carefully chosen, in order to prevent any electrode poisoning reactions since more negative potentials result in a reductive decomposition of the IL. The (electro-)chemical irreversibility of the O_2/O_2^- couple can be attributed to trace impurities [13,45], to a reaction of the IL-cations with the superoxide radicals leading to the corresponding imidazolone [47] (or phosphorus ylide [24] in case of phosphonium cations) or to electrochemical (thermal) decomposition products [48] in the IL that may react with the freshly generated superoxide.

Fig. 3b shows multiple-potential-step-chronoamperometric (MPSC) measurements at different oxygen concentrations. The Pt-sensor-electrode was alternately polarised at 0 V, a potential corresponding to the passage of no Faradaic current (data not shown), and −1.35 V, a potential appropriate to reduce oxygen but not sufficiently negative to poison the electrode. Obviously, the absolute reducing current depends strongly on the amount of oxygen in the gas stream. The sensor showed a response time between 15 and 20 se when switching between the different oxygen concentrations (see also Fig. C in the additional informations. The first sharp peak in Fig. C is assigned to the adjustment of the mass flow controllers. We further assume that the transition between the first and the second (final) current plateau arise because of the developing steady state diffusion current).

Fig. 4a is another demonstration for the correlation of the oxygen concentration of the gas stream and the absolute reducing currents which were measured by an Au-membrane-sensor filled with HMIM

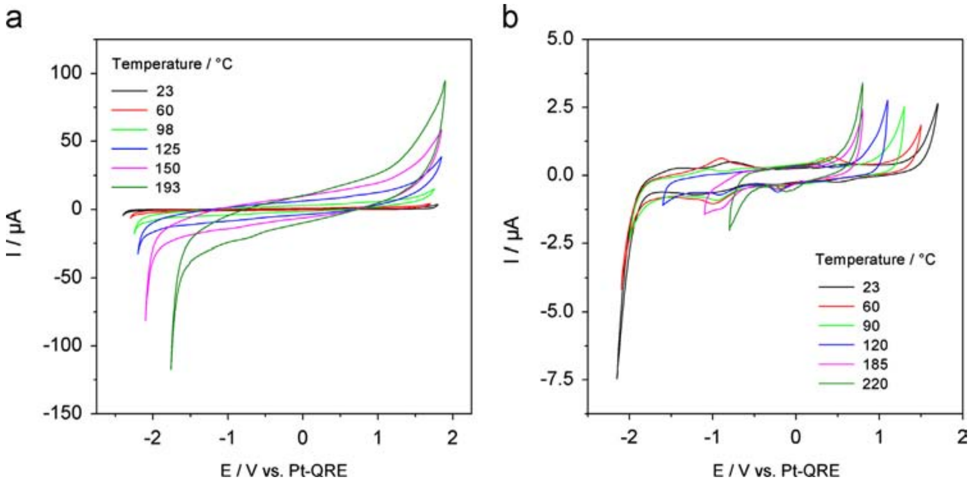

Fig. 2. CVs in OMIM NTf_2 recorded with (a) a GC and (b) a Pt-disk electrode under Ar atmosphere. The active radius was 1 mm and 0.25 mm, respectively, v- 50 mV/s.

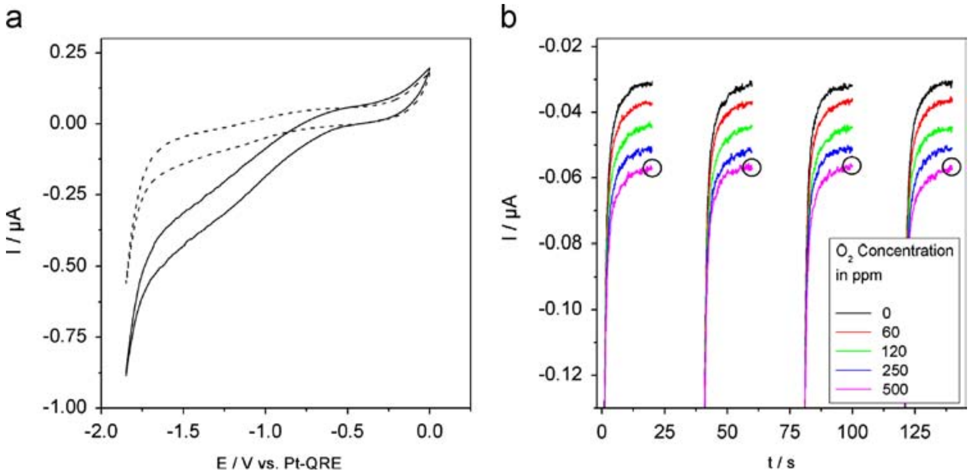

Fig. 3. (a) CVs of a Pt-membrane-sensor (T: 25 °C; sensor electrolyte: HMIM FAP; argon flow rate: 5 L/min) at different oxygen concentrations: 0% oxygen (dotted line) and 0.1% oxygen (straight line). v- 50 mV/s. (b) Chronoamperometrical sensor responses measured at different oxygen concentrations. Same experimental conditions as in (a). The electrode potential was alternately set to $E_1 = 0$ V (20 s, current data not shown) and $E_2 = -1.35$ V (20 s) vs. Pt-QRE. The circles indicate the current values used for the MPSC measurements presented hereafter.

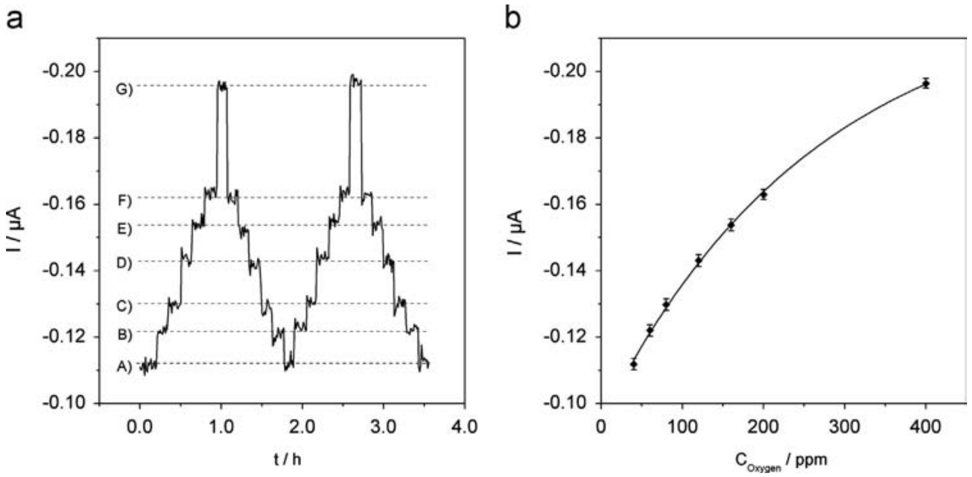

Fig. 4. (a) Current values of a MPSC measurement recorded 20 s after the electrode potential was stepped to an oxygen reducing potential (see circular markings in Fig. 3b) in dependency of the time. The currents were measured by means of an Au-membrane-sensor. (a) T: 29 °C; $E_1 = 0$ V (20 s); $E_2 = -1.35$ V (20 s) vs. Au-QRE; sensor electrolyte: HMIM FAP. Pre-adjusted oxygen concentration in ppm: (A) 40; (B) 60; (C) 80; (D) 120; (E) 160; (F) 200 and (G) 400. Argon flow rate: 5 L/min. (b) Calibration plot: each datapoint represents the mean average of 20–40 measured values shown in (a) in dependency of the oxygen concentration. The error bars express the standard deviation and the straight lines the corresponding theoretical fits. Data were collected from continuous MPSC measurements in varying ppm concentrations of oxygen.

FAP at room temperature. Here, only the current values recorded 20 s after a negative potential step are plotted against the total time of the experiment while changing the oxygen concentration stepwise from 40 to 400 ppm (and vice versa).

Regardless of the different heterogeneous rate constants of the oxygen reduction at gold or platinum electrodes, [22,23,49] there is not a considerable difference between the results of both sorts of sensors. Both electrode materials show a similar dependency between reductive current and oxygen concentration while a too strong polarisation leads to the same poisoning effects. Except of a slight hysteresis the sensor showed reproducible results after several cycles of increasing/decreasing the oxygen concentration. The scattering of the currents in Fig. 4a was indeed so small that the standard deviation of the mean of the currents related to the oxygen content for the time being was negligible. Hence, the resulting calibration plot in Fig. 4b demonstrates excellent sensitivity of the IL-membrane-sensor sufficient for practical use at ambient temperature. As could be expected, it was not linear because the interactions between solvent, electrode surface and redox active species (resulting in possible follow up reactions) change slightly with the analyte concentration, especially in ranges of mere traces of oxygen. The corresponding limit of detection (LOD) for oxygen, based on a signal three times greater than that of the baseline noise (0.005 µA), was 30 ppm. The exponential fit of the calibration has the following equation:

$$I_{red}(\mu A) = -0.225\mu A + 0.130\,\exp\{-0.0038C(O_2)\}$$

where $C(O_2)$ is the concentration of oxygen (in ppm) in oxygen–argon mixture gas. Fig. D in the additional informations shows another MPSC measurement at room temperature of an Au-membrane-sensor filled with EMIM TCB (including calibration plot). Here, the LOD was 5 ppm (baseline noise: 0.01 µA).

3.3. *Cross sensitivity – H_2O*

The reduction of oxygen starts with a one-electron transfer resulting in a superoxide radical anion:

$$O_2 + e^- \rightleftharpoons O_2^- \qquad (2)$$

Savéant et al. described thoroughly several reaction paths of superoxide radical anions reacting with possible Broenstedt acids (including protic solvents). According to their theoretical studies in organic solvents they suggested a subsequent disproportionation mechanism yielding hydrogen peroxide via a two-electron transfer [50].

$$O_2 + 2e^- + 2HA \rightleftharpoons H_2O_2 + 2A^- \tag{3}$$

As previously reported, the mechanism for the reaction of superoxide in ILs in the presence of slight protic impurities and/or water is thought to proceed in the same way. [24,25,45] As the overall reaction mechanism changes from a one to a two-electron transfer, the cathodic peak current is consequently expected to be larger in the presence of water than that under dry conditions. It has to be considered, however, that water affects the properties of ILs in several ways, resulting in a reduction of the electrochemical window, a decreasing viscosity and an enhancement of the mass transport of analyte to the electrode surface [51]. Hence, it is not only the mechanism of the oxygen reduction which changes in the presence of water, but also the diffusion coefficients of the participating species. Taking into account any possible side reactions of the superoxide with the cations of the IL itself it is not surprising that the reductive currents might become hardly reproducible in the presence of water [31,32,45].

Fig. 5a shows CVs of a Pt-electrode in HMIM FAP in a dry and a water saturated oxygen atmosphere. As expected the cathodic peak current increased nearly twice in the humid oxygen atmosphere. The peak observed on the reverse scan may be attributed to the reoxidation of either HO_2 or H_2O_2. Analogue MPSC experiments of an Au-membrane-sensor filled with HMIM FAP in humidified argon–oxygen atmosphere are presented in Fig. 5b. Here, too, the oxygen dependent faradaic response current increased in the presence of humidity. It is not obvious, however, that the currents became less reproducible at the same time. So far, it was not possible to work with a membrane-sensor under humid conditions for more than two days.

3.4. Cross sensitivity – CO_2

Electrochemical reactions in ILs can be strongly influenced by CO_2. Barosse-Antle et al. demonstrated successfully that the mere presence of CO_2 is sufficient to decrease the diffusional and rotational activation energy of ferrocene in EMIM NTf_2 (resulting in an enhancement of the oxidation current of 110%) [52]. Indeed, the impact of CO_2 on the oxygen reduction depends strongly on the temperature, the concentration of oxygen and CO_2 as well as on the IL serving as electrolyte.

Fig. 6a presents CVs of a Pt-electrode in HMIM FAP under a blanket of argon (dotted line), oxygen–argon (50:50, dashed line) and oxygen-CO_2 (50:50, straight line). Meanwhile the CV indicated an irreversible one electron transfer in the presence of argon and oxygen according to Eq. (2), the mechanism changed completely in the presence of CO_2. Here, the cathodic peak current values increased twice, whereas the anodic peak vanished completely. It is commonly accepted that this behaviour can be explained by switching from the one electron reduction of oxygen to the overall two electron process for the reaction of superoxide with CO_2 [53].

$$O_2 + 2e^- + CO_2 \rightleftharpoons C_2O_6^{2-} \tag{4}$$

Depending on the IL, Buzzeo et al. suggested an ECE or a disproportionation mechanism, i.e. the electrogenerated superoxide anion reacts with CO_2 [49]. Chemical follow-up reactions of the resulting CO_4 radical anion with CO_2 and superoxide (yielding peroxodicarbonate) finally lead to an encreased number of transferred electrons accompanied by an irreversible reaction mechanism.

Fig. 6b is another demonstration of a MPSC experiment using an Au-membrane-sensor filled with HMIM FAP. Again, the sensor reply was stable and reproducible in the absence of CO_2 (first and second variation cycle). Switching the oxygen concentration in the presence of 2800 ppm CO_2 altered the situation distinctly, i.e. the reductive currents increased in accordance with the CVs shown in Fig. 6a and a strong hysteresis appeared.

An influence of CO_2 upon any oxygen reducing currents was also noticed using Pt-sensor-electrodes. Fig. E in the supplementary data shows MPSC results of a Pt-membrane-sensor filled with EMIM NTf_2. Analogue to Fig. 6b any variation of the oxygen concentration in the absence of CO_2 resulted once more in a reproducible and strictly oxygen dependent current signal. As soon as the carrier gas contained even mere traces of CO_2 the current augmented drastically. Changing the CO_2 concentration from 180 to 2800 ppm (at a constant oxygen concentration of 40 ppm), however, did not alter the current noticeably and resulted in a constant current plateau.

Whereas the oxygen reduction is distinctly influenced by humidity and CO_2 because of changes of the solvents properties as well as the reaction mechanism, further complications are to be anticipated in the presence of hydrogen sulphide and sulphur dioxide owing to a

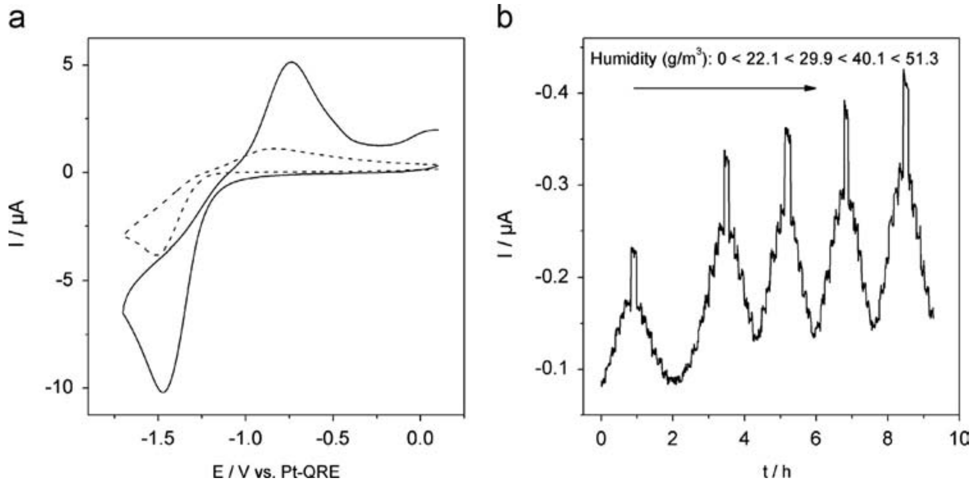

Fig. 5. (a) CVs of a Pt-disk electrode (r: 0.25 mm) in HMIM FAP under a blanket of dry oxygen (dotted line) and of water saturated oxygen (straight line); T: 25 °C; v- 350 mV/s. (b) Current values of a MPSC measurement in dependency of the time (experimental conditions and oxygen concentrations see Fig. 4a). The currents were measured in a gas stream of different humidities. T: 23 °C.

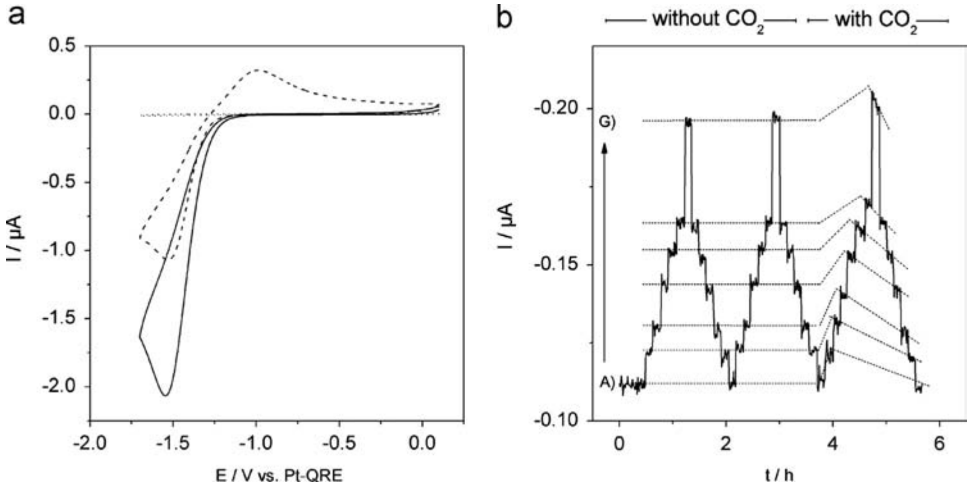

Fig. 6. (a) CVs of a Pt-disk electrode (r: 0.25 mm) in HMIM FAP under a blanket of argon (dotted line), of oxygen:argon 50:50 (dashed line) and of oxygen:CO_2 50:50 (straight line); v- 50 mV/s, T: 22 °C. (b) Current values of a MPSC measurement in dependency of the time (experimental conditions see Fig. 4a). The variation of the oxygen content started in the absence of CO_2 (first and second variation cycle). The final variation cycle was recorded under the same conditions as cycle one and two in the presence of 2800 ppm CO_2.

similar redox potential of these two analytes and oxygen itself [54–56]. Up to now no satisfactory solution can be offered to exclude these cross sensitivities.

3.5. *Long-term behaviour*

A closer look at Fig. 4a reveals a very slight drift of the sensor signal. Such a drift appears occasionally if the sensor was not polarised long enough. Most of the times, it took the sensor electrodes about 18 h to reach a constant state of electrochemical equilibrium (because of adsorption layers, traces of oxygen in the membrane etc.) so that the values of the current signal remained constant. Long-time investigations, however, look positively encouraging. The black line in Fig. 7 represents the reducing currents recorded over a week in a MPSC experiment by the same sensor which was used in Fig. E (supplementary data). A corresponding current reply of the secondary electron multiplier of a reference mass spectrometer (MS) is displayed by a line of *x*-symbols. The IL-sensor current agreed well with the MS-control signal confirming the pre-adjusted gas contents. It shows a constant oxygen concentration of 193 ± 25 ppm (set point: 160 ppm) interrupted three times by a concentration shift towards 71 ± 16, 113 ± 11 and 71 ± 16 ppm (set points: 80, 120 and 80 ppm). An analogue positive shift of the upper concentration can also be found in the MS data. A reason for such a deviation might be a lower flow rate of the carrier gas (1 L/min) which enables an intrusion of traces of oxygen. Nevertheless, the sensor signal turned out to be rather stable apart from three bulges after increasing the oxygen concentration which look like a temporal damping effect. Moreover, both signals show periodical deviations over the first 5 days. This can be explained easily by the night and day oscillations of the surrounding temperature (which influences the IL's conductivity and the pressure in the gas mixing device) and is another hint for the strong sensitivity of the IL-membrane-sensor.

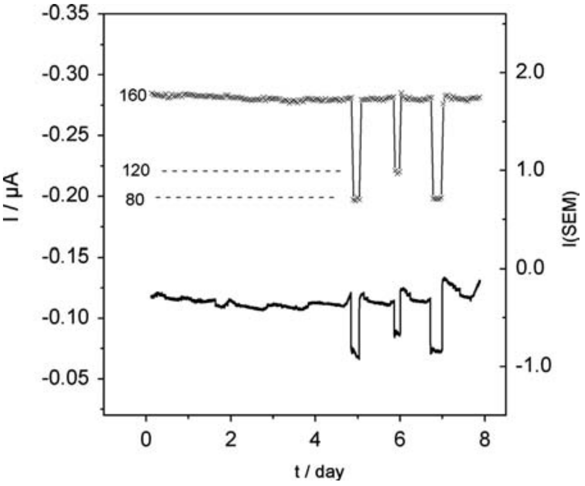

Fig. 7. Current values of a MPSC measurement in dependency of the time (see Fig. 4) – recorded over a period of 8 days. The currents were measured by means of a Pt-membrane-sensor. T: 23 °C; E_1=0 V (20 s); E_2=-1.35 V (20 s); sensor electrolyte: EMIM NTf_2. Black line: current of the EMIM NTf_2 membrane-sensor, *x*-symbols: signal of a controlling mass spectrometer.

3.6. *Thermal behaviour*

Meanwhile the sensor signal for any sensor filled with EMIM NTf_2, EMIM TCB and HMIM FAP was rather reproducible at room temperature, the situation changed completely using $P_{6,6,6,14}$ NTf_2 as electrolyte. Because of the thermal stability at higher temperatures of the phosphonium IL, latter would have been an extremely interesting candidate for high temperature applications. We assume a high viscosity and an apparent disadvantageous wetting behaviour being responsible for very low sensor currents, which were extremely susceptible for electrical noise – even at room temperature.

Fig. F in the supporting data shows the results of an MPSC measurement at 126 °C obtained by the same HMIM FAP filled sensor used for the measurement presented in Fig. 4a. Again, the sensor current depends strongly on the oxygen concentration. As the viscosity decreases at elevated temperatures the absolute currents are slightly higher compared to those measured at room temperature. Voltammographic measurements of the sensor at room temperature and 126 °C (data not shown) showed a slight positive shift of the reduction potentials which is most likely due to a faster kinetics at elevated temperatures. The MPSC measurements were recorded, therefore, at − 1.2 V (instead of − 1.35 V like at room temperature). Thus, the sensor potential should be adjusted in dependence of the temperature in order to avoid a falsification of the sensor results and a possible destruction of the

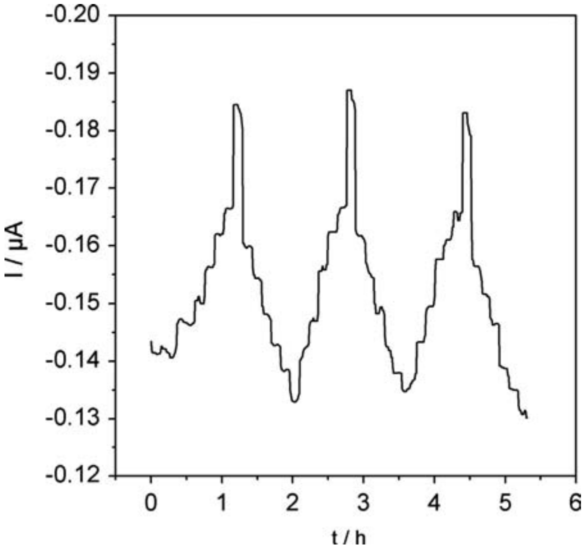

Fig. 8. Current values of a MPSC measurement of two Au-membrane-sensors in dependency of the time (see Fig. 4a). Sensor electrolyte: HMIM FAP; same experimental conditions as before. T: 163 °C; $E_1=0$ V (20 s); $E_2=-0.9$ V (20 s).

IL. Furthermore, a characteristical hysteresis-behaviour made a modelling of a calibration curve very difficult. Fig. 8 represents analogue results obtained by another Au-membrane-sensor (filled with HMIM FAP, too) at 163 °C. As the currents were easily affected by electrical noise the results were smoothed using a percentile $Q_{.5}$ filter. If an alternating oxygen concentration is applied to the sensor its reducing current traced out a loop again. An explanation for such a hysteresis-behaviour might be surface reactions which take place in particular at higher oxygen concentrations and temperatures causing electrode poisoning reactions and passivating adlayers which apparently disappear when the oxygen concentration is decreased again.

4. Conclusion

We have successfully developed amperometric oxygen sensors based on IL-supported ceramic membranes for trace analysis. The sensors are easily constructed and yield a detection limit as low as 5 ppm at 25 °C, a high sensitivity and a rapid response time. The present IL-based sensors can be continuously used for at least one week with the operation of multiple-potential-step-chronoamperometry. At elevated temperatures, it was still possible to detect oxygen in the ppm range, but the sensors suffered strongly from hysteresis and irreproducible behaviour – probably because of electrode poisoning reactions.

Further investigations in the presence of humidity and CO_2 proved significant but hardly predictable cross sensitivities, as a result of which the sensor currents usually increased and became less reproducible. Apparently, these interferences originate in a mechanistic change of the oxygen reduction.

Electrochemical investigations of various ILs between 20 and 220 °C demonstrated a superior conductivity of TCB based ILs compared to their NTf_2 and FAP based analogues. Apart from the conductivity, the potential window is of crucial importance, though. Voltammetric characterisations in the same temperature range underlined the catalytic activity of Pt-electrodes compared to GC-electrodes and showed potential windows, all of which tended to be very susceptible to temperature. According to these results, the application of ILs (as sensor electrolytes) at elevated temperatures is often limited and depends on the electrode material, the gas solubility and the redox potential of the analyte in question.

All in all, first investigations indicate that the new sensor-concept can be applied to the trace analysis of oxygen (and presumably other target gases) at room temperature under consideration of possible cross sensitivities. High temperature applications, however, might require the development of new electrode materials. Further research on this contribution would be of value and is in hand.

Appendix A. Supporting information

Supplementary data associated with this article can be found in the online version at http://dx.doi.org/10.1016/j.talanta.2013.07.001.

Reference

[1] C.W. Chen, S.C. Hung, M.D. Yang, C.W. Yeh, C.H. Wu, G.C. Chi, F. Ren, S. J. Pearton, Oxygen sensors made by monolayer graphene under room temperature, Appl. Phys. Lett. 99 (2011).
[2] Y. Gurbuz, W.P. Kang, J.L. Davidson, D.V. Kerns, High temperature tolerant diamond-based microelectronic oxygen gas sensor, Sensors Actuators B–Chem. 49 (1998) 115–120.
[3] Y. Miyahara, K. Tsukada, H. Miyagi, Field-effect transistor using a solid electrolyte as a new oxygen sensor, J. Appl. Phys. 63 (1988) 2431–2434.
[4] G. Alberti, A. Carbone, R. Palombari, Oxygen potentiometric sensors based on thermally stable solid state proton conductors: a preliminary investigation in the temperature range 150–200 °C, Sensors Actuators B–Chem. 86 (2002) 150–154.
[5] N. Izu, W. Shin, I. Matsubara, N. Murayama, N. Oh-hori, M. Itou, Temperature independent resistive oxygen sensors using solid electrolyte zirconia as a new temperature compensating material, Sensors Actuators B–Chem. 108 (2005) 216–222.
[6] M. Ogita, K. Higo, Y. Nakanishi, Y. Hatanaka, Ga_2O_3 thin film for oxygen sensor at high temperature, Appl. Surf. Sci. 175–176 (2001) 721–725.
[7] Z. Peng, M. Liu, E. Balko, A new type of amperometric oxygen sensor based on a mixed-conducting composite membrane, Sensors Actuators B–Chem. 72 (2001) 35–40.
[8] A. Rothschild, S.J. Litzelman, H.L. Tuller, W. Menesklou, T. Schneider, E. Ivers-Tiffee, Temperature-independent resistive oxygen sensors based on SrTi(1 − x)Fe(x)O(3-delta) solid solutions, Sensors Actuators B–Chem. 108 (2005) 223–230.
[9] Physical chemistry of ionic liquids, Phys.Chem.Chem.Phys., 12, 2010.
[10] P. Wasserscheid, T. Welton, IonicLiquids in Synthesis, Wiley-VCH Verlag GmbH, Weinheim, 2008.
[11] H. Ohno, Electrochemical Aspects of Ionic Liquids, John Wiley and Sons, Inc., Hoboken, New Jersey, 2005.
[12] J.L. Anthony, J.L. Anderson, E.J. Maginn, J.F. Brennecke, Anion effects on gas solubility in ionic liquids, J. Phys. Chem. B 109 (2005) 6366–6374.
[13] M.C. Buzzeo, R.G. Evans, R.G. Compton, Non-haloaluminate room-temperature ionic liquids in electrochemistry–a review, ChemPhysChem 5 (2004) 1106–1120.
[14] M.C. Buzzeo, C. Hardacre, R.G. Compton, Use of room temperature ionic liquids in gas sensor design, Anal.Chem. 76 (2004) 4583–4588.
[15] M.C. Buzzeo, O.V. Klymenko, J.D. Wadhawan, C. Hardacre, K.R. Seddon, R.G. Compton, Voltammetry of oxygen in the room-temperature ionic liquids 1-Ethyl-3-methylimidazolium Bis((trifluoromethyl)sulfonyl)imide and Hexyltriethylammonium Bis((trifluoromethyl)sulfonyl)imide: one-electron reduction to form superoxide. steady-state and transient behaviour in the same cyclic voltammogram resulting from widely different diffusion coefficients of oxygen and superoxide, J. Phys. Chem. A 107 (2003) 8872–8878.
[16] M. Hayyan, F.S. Mjalli, M.A. Hashim, I.M. AlNashef, X.M. Tan, Electrochemical reduction of dioxygen in Bis (trifluoromethylsulfonyl) imide based ionic liquids, J. Electroanal. Chem. 657 (2011) 150–157.
[17] J. Jacquemin, M.F.C. Gomes, P. Husson, V. Majer, Solubility of carbon dioxide, ethane, methane, oxygen, nitrogen, hydrogen, argon, and carbon monoxide in 1-butyl-3-methylimidazolium tetrafluoroborate between temperatures 283 K and 343 K and at pressures close to atmospheric, J. Chem. Thermodyn. 38 (2006) 490–502.
[18] J. Jacquemin, P. Husson, V. Majer, M.F.C. Gomes, Low-pressure solubilities and thermodynamics of solvation of eight gases in 1-butyl-3-methylimidazolium hexafluorophosphate, Fluid Phase Equilibria 240 (2006) 87–95.
[19] J. Kumelan, A.P.S. Kamps, I. Urukova, D. Tuma, G. Maurer, Solubility of oxygen in the ionic liquid [bmim][PF6]: experimental and molecular simulation results, J. Chem. Thermodyn. 37 (2005) 595–602.
[20] J. Kumelan, A.P.S. Kamps, D. Tuma, G. Maurer, Solubility of the single gases carbon monoxide and oxygen in the ionic liquid [hmim][Tf_2N], J. Chem. Eng. Data 54 (2009) 966–971.

[21] A.S. Barnes, E.I. Rogers, I. Streeter, L. Aldous, C. Hardacre, G.G. Wildgoose, R.G. Compton, Unusual voltammetry of the reduction of O-2 in [C(4)dmim][N(Tf)(2)] reveals a strong interaction of O-2(center dot-) with the [C(4)dmim](+) cation, J. Phys. Chem. C 112 (2008) 13709–13715.
[22] X.J. Huang, E.I. Rogers, C. Hardacre, R.G. Compton, The reduction of oxygen in various room temperature ionic liquids in the temperature range 293-318 K: exploring the applicability of the stokes-einstein relationship in room temperature ionic liquids, J. Phys. Chem. B 113 (2009) 8953–8959.
[23] E.I. Rogers, X.J. Huang, E.J.F. Dickinson, C. Hardacre, R.G. Compton, Investigating the mechanism and electrode kinetics of the oxygen vertical bar superoxide (o-2 vertical bar o-2(center dot-)) couple in various room-temperature ionic liquids at gold and platinum electrodes in the temperature range 298-318 K, J. Phys. Chem. C 113 (2009) 17811–17823.
[24] R.G. Evans, O.V. Klymenko, S.A. Saddoughi, C. Hardacre, R.G. Compton, Electroreduction of oxygen in a series of room temperature ionic liquids composed of group 15-centered cations and anions, J. Phys. Chem. B 108 (2004) 7878–7886.
[25] Y. Katayama, H. Onodera, M. Yamagata, T. Miura, Electrochemical reduction of oxygen in some hydrophobic room-temperature molten salt systems, J. Electrochem. Soc. 151 (2004) A59–A63.
[26] J. Ghilane, C. Lagrost, P. Hapiot, Scanning electrochemical microscopy in nonusual solvents: inequality of diffusion coefficients problem, Anal. Chem. 79 (2007) 7383–7391.
[27] Z. Wang, P. Lin, G.A. Baker, J. Stetter, X. Zeng, Ionic liquids as electrolytes for the development of a robust amperometric oxygen Sensor, Anal. Chem. 83 (2011) 7066–7073.
[28] N. Dossi, R. Toniolo, A. Pizzariello, E. Carrilho, E. Piccin, S. Battiston, G. Bontempelli, An electrochemical gas sensor based on paper supported room temperature ionic liquids, Lab Chip 12 (2012) 153–158.
[29] X.J. Huang, L. Aldous, A.M. O'Mahony, F.J. del Campo, R.G. Compton, Toward membrane-free amperometric gas sensors: a microelectrode array approach, Anal. Chem. 82 (2010) 5238–5245.
[30] S.Q. Xiong, Y. Wei, Z. Guo, X. Chen, J. Wang, J.H. Liu, X.J. Huang, Toward membrane-free amperometric gas sensors: an ionic liquid nanoparticle composite approach, J. Phys. Chem. C 115 (2011) 17471–17478.
[31] R. Wang, S. Hoyano, T. Ohsaka, O_2 Gas sensor using supported hydrophobic room-temperature ionic liquid membrane-coated electrode, Chem. Lett. 33 (2004) 6–7.
[32] R. Wang, T. Okajima, F. Kitamura, T. Ohsaka, A novel amperometric O-2 gas sensor based on supported room-temperature ionic liquid porous polyethylene membrane-coated electrodes, Electroanalysis 16 (2004) 66–72.
[33] X.X. Jin, L. Yu, D. Garcia, R.X. Ren, X.Q. Zeng, Ionic liquid high-temperature gas sensor array, Anal. Chem. 78 (2006) 6980–6989.
[34] A. Smie, A. Synowczyk, J. Heinze, R. Alle, P. Tschuncky, G. Goetz, P. Baeuerle, beta, beta-Disubstituted oligothiophenes, a new oligomeric approach towards the synthesis of conducting polymers, J. Electroanal. Chem. 452 (1998) 87–95.
[35] P. Bonhote, A.P. Dias, M. Armand, N. Papageorgiou, K. Kalyanasundaram, M. Gratzel, Hydrophobic, highly conductive ambient-temperature molten salts (vol. 35, p. 1168, 1996), Inorg. Chem. 37 (1998) 166.
[36] N.V. Ignat'ev, U. Welz-Biermann, A. Kucheryna, G. Bissky, H. Willner, New ionic liquids with tris(perfluoroalkyl)trifluorophosphate (FAP) anions, J. Fluorine Chem. 126 (2005) 1150–1159.
[37] H.L. Ngo, K. LeCompte, L. Hargens, A.B. McEwen, Thermal properties of imidazolium ionic liquids, Thermochim. Acta 357 (2000) 97–102.
[38] J.O. Valderrama, P.A. Robles, Critical properties, normal boiling temperatures, and accentric and factors of fifty ionic liquids, Industrial and Engineering Chemistry Research 46 (2007) 1338–1344.
[39] J.M. Pringle, J. Golding, K. Baranyai, C.M. Forsyth, G.B. Deacon, J.L. Scott, D. R. MacFarlane, The effect of anion fluorination in ionic liquids – physical properties of a range of bis(methanesulfonyl)amide salts, New J. Chem. 27 (2003) 1504–1510.
[40] F. Endres, O. Hofft, N. Borisenko, L.H. Gasparotto, A. Prowald, R. Al-Salman, T. Carstens, R. Atkin, A. Bund, S. Zein El Abedin, Do solvation layers of ionic liquids influence electrochemical reactions? Phys. Chem. Chem. Phys. 12 (2010).
[41] H.T. Liu, Y. Liu, J.H. Li, Ionic liquids in surface electrochemistry, Phys. Chem. Chem. Phys. 12 (2010) 1685–1697.
[42] R.G. Evans, O.V. Klymenko, C. Hardacre, K.R. Seddon, R.G. Compton, Oxidation of N,N,N',N'-tetraalkyl-para-phenylenediamines in a series of room temperature ionic liquids incorporating the bis(trifluoromethylsulfonyl)imide anion, J. Electroanal. Chem. 556 (2003) 179–188.
[43] U. Schroder, J.D. Wadhawan, R.G. Compton, F. Marken, P.A.Z. Suarez, C.S. Consorti, R.F. de Souza, J. Dupont, Water-induced accelerated ion diffusion: voltammetric studies in 1-methyl-3-[2,6-(S)-dimethylocten-2-yl]imidazolium tetrafluoroborate, 1-butyl-3-methylimidazolium tetrafluoroborate and hexafluorophosphate ionic liquids, New J. Chem. 24 (2000).
[44] M.V. Migliorini, R.K. Donato, M.A. Benvegnu, J. Dupont, R.S. Goncalves, H.S. Schrekker, Imidazolium ionic liquid-water mixtures: the formation of a new species that inhibits the electrocatalytical charge transfer processes on a platinum surface, Catal. Commun. 9 (2008) 971–975.
[45] I.M. AlNashef, M.L. Leonard, M.C. Kittle, M.A. Matthews, J. Weidner, Electrochemical generation of superoxide in room-temperature ionic liquids, Electrochem. Solid-State Lett. 4 (2001) D16–D18.
[46] I.M. AlNashef, M.L. Leonard, M.A. Matthews, J.W. Weidner, Superoxide electrochemistry in an ionic liquid, Ind. Eng. Chem. Res. 41 (2002) 4475–4478.
[47] I.M. AlNashef, M.A. Hashim, F.S. Mjalli, M.Q.A. Ali, M. Hayyan, A novel method for the synthesis of 2-imidazolones, Tetrahedron Lett. 51 (2010) 1976–1978.
[48] M. Sobota, M. Schmid, M. Happel, M. Amende, F. Maier, H.P. Steinruck, N. Paape, P. Wasserscheid, M. Laurin, J.M. Gottfried, J. Libuda, Ionic liquid based model catalysis: interaction of [BMIM][Tf_2N] with Pd nanoparticles supported on an ordered alumina film, Phys. Chem. Chem. Phys. 12 (2010) 10610–10621.
[49] M.C. Buzzeo, O.V. Klymenko, J.D. Wadhawan, C. Hardacre, K.R. Seddon, R.G. Compton, Kinetic analysis of the reaction between electrogenerated superoxide and carbon dioxide in the room temperature ionic liquids 1-ethyl-3-methylimidazolium bis(trifluoromethylsulfonyl)imide and hexyltriethylammonium bis(trifluoromethylsulfonyl)imide, J. Phys. Chem. B 108 (2004) 3947–3954.
[50] C.P. Andrieux, P. Hapiot, J.M. Saveant, Mechanism of superoxide ion disproportionation in aprotic-solvents, J. Am. Chem. Soc. 109 (1987) 3768–3775.
[51] A.M. O'Mahony, D.S. Silvester, L. Aldous, C. Hardacre, R.G. Compton, Effect of water on the electrochemical window and potential limits of room-temperature ionic liquids, J. Chem. Eng. Data 53 (2008) 2884–2891.
[52] L.E. Barrosse-Antle, C. Hardacre, R.G. Compton, Voltammetric currents in room temperature ionic liquids can reflect solutes other than the electroactive species and are influenced by carbon dioxide, J. Phys. Chem. B 113 (2009) 2805–2809.
[53] I.M. AlNashef, M.L. Leonard, M.A. Matthews, J.W. Weidner, Superoxide electrochemistry in an ionic liquid, Ind. Eng. Chem. Res. 41 (2002) 4475–4478.
[54] A.M. O'Mahony, E.J.F. Dickinson, L. Aldous, C. Hardacre, R.G. Compton, Electrochemical oxidation of hydrogen sulphide at platinum electrodes in room temperature ionic liquids: evidence for significant accumulation of H2S at the Pt/1-Butyl-3-methylimidazolium trifluoromethylsulfonate interface, J. Phys. Chem. C 113 (2009) 10997–11002.
[55] A.M. O'Mahony, D.S. Silvester, L. Aldous, C. Hardacre, R.G. Compton, The electrochemical reduction of hydrogen sulphide on platinum in several room temperature ionic liquids, J. Phys. Chem. C 112 (2008) 7725–7730.
[56] L.E. Barrosse-Antle, D.S. Silvester, L. Aldous, C. Hardacre, R.G. Compton, Electroreduction of sulphur dioxide in some room-temperature ionic liquids, J. Phys. Chem. C 112 (2008) 3398–3404.